論文 / 著書情報
Article / Book Information

Title	Ray-based and wavefront-based holographic displays for high-density light-field reproduction
Authors	Masahiro Yamaguchi
Citation(English)	Proc. SPIE, Vol. 8043, ,
発行日 / Pub. date	2011, 4
DOI	10.1117/12.884500
権利情報 / Copyright	本著作物の著作権はSociety of Photo-Optical Instrumentation Engineersに帰属します。 Copyright 2011 Society of Photo-Optical Instrumentation Engineers. One print or electronic copy may be made for personal use only. Systematic reproduction and distribution, duplication of any material in this paper for a fee or for commercial purposes, or modification of the content of the paper are prohibited.

Ray-based and wavefront-based holographic displays for high-density light-field reproduction

Masahiro Yamaguchi
Global Scientific Information and Computing Center, Tokyo Institute of Technology,
2-12-1-I7-6 Ookayama, Meguro-ku, Tokyo, 152-8550, JAPAN

ABSTRACT

This paper introduces holographic 3D displays for ray-based and wavefront-based light-field reproductions. As a ray-based display though a hard copy 3D image, a holographic 3D printer is introduced, which automatically outputs high-resolution full-parallax holographic stereograms from 3D image data. Fine-quality full-color 3D images were experimentally obtained with excellent gloss and texture appearances. As a wavefront-based display, we have proposed a technique for calculating computer generated hologram, in which the wavefront is derived from the light-ray information. High-resolution display of deep 3D scene is possible, while realistic image can be generated by utilizing conventional rendering techniques for computer graphics.

Keywords: 3D display, light-field display, holography, holographic stereogram, computer generated hologram,

1. INTRODUCTION

In the future of 3D displays, the optical reproduction of light-field [1] is promising because it enables to produce highly realistic 3D images. Based on the holographic technique, high-density light-field can be presented and natural 3D image can be observed with all the depth cues, such as binocular parallax, motion parallax, and accommodation. This paper demonstrates two different approaches for 3D display with high-density light-field reproduction; ray-based and wavefront-based techniques.

As a ray-based display though a hard copy 3D image, the first part of this paper introduces a holographic 3D printer [2,3], which automatically outputs high-resolution full-parallax (FP) holographic stereogram (HS) from 3D image data. HS is a 3D display, in which 2D images with parallax are recorded with holographic technique so that stereoscopic images can be observed without using glasses [4]. HS presents parallax information with multi-view images, and an observer perceives depth with binocular disparity and motion parallax. However, if we increase the number of views in HS, it can be considered as a display that reconstructs light-rays from the object. An advantage of HS compared to other autostereoscopic displays is the capability of recording high-density light-rays, or light-field, since HS does not require either parallax barrier or lenticular lens sheet. High-quality full-color 3D images were experimentally obtained with excellent gloss and texture appearances [3].

However, there is a limitation in ray-based displays, i.e., the resolution of the image far from the display plane is degraded. The wavefront-based holographic display is thus expected to breakthrough such limitation for deep 3D image reproduction. For this purpose, the techniques of computational holography, or computer generated hologram (CGH) is promising. A typical method for calculating CGH for 3D display is synthesizing spherical waves propagating from a set of point sources defined on the object surface [5,6]. It simulates physical phenomena of electromagnetic wave propagation and high resolution image can be reproduced even in the case of deep 3D scene. However it is not easy to deal with occlusion and surface reflection property, which are vital in realistic 3D display. Another approach is based on light-ray recording and reproduction [7,8], in other words, CGH that reconstructs high-density light-rays. In this approach, advanced rendering techniques for 3D graphics, including ray-tracing, image-based rendering can be employed for generating hologram fringe. But the spatial resolution decreases in the reconstructed image located far from the display plane, due to the sampling of light-rays and the diffraction limit. Therefore we have proposed a new method for hologram computation that takes the advantages of those wavefront-based and ray-ba Z hes. This method enables reproducing deep 3D images without resolution degradation even though the wavefront is generated from ray information. In the method, the light-

*yamaguchi.m.aa@m.titech.ac.jp; phone 81 3 5734 3653; fax 81 3 5734-3276; http://guchi.gsic.titech.ac.jp

rays are sampled numerically at a ray-sampling (RS) plane defined near the image location, and they are transformed to the wavefront by using Fourier transforms. Then the wavefront propagation is calculated based on the diffraction theory, resulting in high-resolution display of deep 3D scene, while realistic image is obtained from the light-ray information calculated by conventional rendering techniques for computer graphics. The experimental results of both ray-based and wavefront-based 3D displays are demonstrated by the printed holograms.

In this paper, the future trends of holographic 3D displays are discussed in section 2 to discuss what should we set our sights on. Section 3 introduces an example of 3D display with high-density light-field, recorded by a holographic 3D printer. In section 4, a method for wavefront-based light-field reproduction using RS plane is described, as well as the experimental results obtained by using CGH printer. Section 5 summarizes this article.

2. FUTURE TRENDS OF HOLOGRAPHIC 3D DISPLAY

For holographic 3D display huge amount of data must be presented. In hardcopy 3D display it is possible to sequentially record such huge information, but electronic holographic display, or electro-holography requires much more efforts to be realized. The information necessary for holographic display is quite huge, the advancements are needed in both processing and displaying such huge information. Especially the spatio-temporal resolution of display device is a critical issue. A well-known method to reduce the data amount is discarding vertical parallax, namely, horizontal-parallax only (HPO) hologram approach. However, the specifications of recent autostereoscopic 3D displays have been amazingly advanced, and their image quality is becoming nearly comparable to HPO hologram. So, what is a unique feature of holography? What kind of 3D image can we expect for holography?

One of the important points is visual fatigue, caused by the inconsistent depth cues between binocular disparity and the focus in binocular stereo or multi-view 3D displays. Holography is expected to solve the problem, since all the depth cues are satisfied. In addition, it is known that holography can reproduce realistic 3D image of very deep 3D scene. Image display of deep 3D scene is affected by the image blur in conventional autostereoscopic displays such as lenticular or parallax-barrier displays. Therefore, one of the visions of the future of holographic 3D display is illustrated in fig.1; another world is appeared beyond the window of display, though some object can be appeared in near side, such as another room, office, city, or natural scene. An observer can see the display not only from a certain distance from the display plane, but from the close proximity of the display. This fact also leads an additional feature of holography; large image can be observed even in small display, if viewing from very close to the display.

Next question thus is what specifications are required to display device? According to previous studies on the requirements to the holographic display device, the specification of a holographic display can be roughly determined by 1) hologram size (D) and 2) viewing angle or the angle of viewing field (θ). We can employ an optical system that magnifies the image size, but if we magnify the image size of hologram, the viewing angle becomes small. In fact, the product $D \times \theta$ is constant if the number of pixels in one dimension, referred to N, is fixed, or, approximately $D \times \theta = N \lambda$. Therefore the most critical requirement is the number of pixels. For example, to reproduce a human subject in a virtual window of 2.0 m height located at 1.0 m from the display, the viewing angle should be almost 90 degrees. In case of bust shot it becomes about 30 degrees. If the display size is 10 inch diagonal (aspect ratio 4:3), and the viewing angle is 30 degrees and full-parallax, the number of pixels becomes about 207,000 × 155,000. Assuming 30Hz refresh rate, then the total number of pixels required for this display is almost 9.6×10^{11} pixels/second. Higher specification one, 40 inch diagonal display (aspect ratio 16:9) with viewing angle 90 degrees, requires 2,500,000 × 1,400,000 pixels and 1.0×10^{14} pixels/second in 30Hz refresh rate. In short, a display device that is capable of presenting about $10^{12} \sim 10^{14}$ pixels/second is required for holographic display.

Now the final question is, when can we see the holographic display? Let us briefly take a look at the history of display devices for non-military purposes. In 1988, Epson commercialized liquid crystal television of 320×220 pixels, 30 f/s, which corresponds to 2.1×10^6 pixels/second. In mid 1990's, VGA (640×480 pixels) display which is almost equivalent to NTSC television was commonly available. High-definition (1920×1080 pixels, 60 f/s $\cong 1.2 \times 10^8$ pixels/second) liquid crystal display (LCD) was presented around 1999, 4k in mid 2000's, and recently 8k LCoS projector has been announced; 8192×4320 pixels, 60 f/s $\cong 2.1 \times 10^9$ pixels/second. High-speed MEMS display, for example digital micromirror device (DMD) of 1920×1080 pixels, 24 kHz (binary image) is now available. Fig. 2 shows the plot of the progress of the display devices. We can see the trend similar to the Moore's law. Although this is quite rough estimate and there is no evidence that support the validity of future extrapolation, the discussion here suggest that in mid-2020's, the device suitable for holographic display will be available.

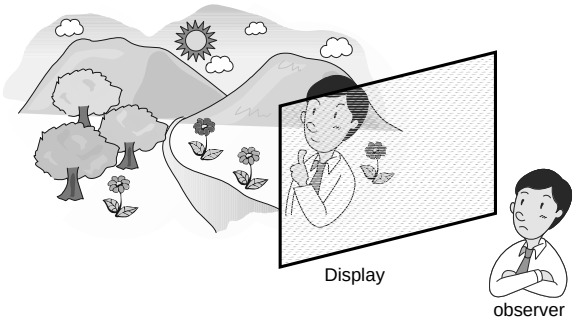

Fig.1 An example of holographic display in future. Very deep scene appears and the display is similar to window to another world.

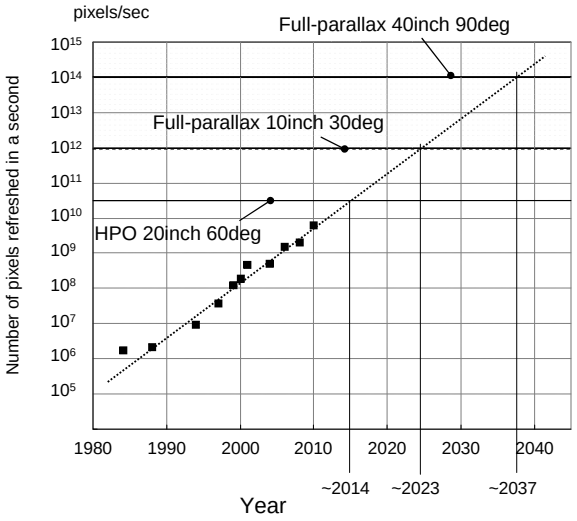

Fig.2 The trend of spatio-temporal resolution (pixels/ second) of display devices from late1980's to 2010. Square dots represent examples of commercialized or prototyped display devices. Horizontal lines denote the resolutions required for holographic displays of several specifications. Predicted line was hand-written.

3. RAY-BASED HOLOGRAPHIC DISPLAY FOR HIGH-DENSITY LIGHT-FIELD REPRODUCTION

3.1 Holographic 3D printer

A holographic 3D printer was originally proposed on 1990 [2], in which the technique for automatic recording of full-parallax (FP) HS was used. Contrary to the autostereoscopic displays with HPO, FP-HS enables the observation of distortion-free 3D images from arbitrary location within the viewing zone. HPO hologram printers [10)] have been studied by MIT Media Lab. [11], Dutch Holographics [12] and Sony [13] in 1990's, and Zebra Inc. commercialized the technology of FP-HS [14]. The author's group has been focused on the high-density recording of light-rays, and achieved spatial resolution 50 - 200μm and angular resolution ≅ 0.3 degree in full-color FP-HS [3,15].

3.2 Full-parallax holographic stereogram

In recording FP-HS, first a set of images for exposure is prepared using graphics technique such as ray-tracing or image-based rendering. Fig.3(a) shows the geometry of generating the image for exposure. A hologram plane is defined at arbitrary location around the object, and a 2D sampling grid is also defined on the hologram plane. An image for exposure is generated by projecting 3D objects where the center of projection is every sample point of the sampling grid on the hologram plane.

In the recording step of hologram, the image for exposure is displayed on a spatial light modulator such as liquid crystal display (LCD) in the optical system shown in fig.3(b). The LCD is illuminated by a plane wave from a laser light source, and an objective lens converts the plane wave to converging spherical wave. The holographic recording medium is placed approximately at the focal plane of the objective lens, and combining with the reference beam that come from the opposite side, the interference pattern is recorded in a small area around the grid point on the holographic recording medium. The small hologram is called elementary hologram (sometimes called "hogel" [14]). A weak diffuser is inserted near the LCD panel to suppress the intensity variation of object beam on the hologram plane. After the exposure of an elementary hologram, the recording medium is moved at a pitch to horizontal / vertical direction for next exposure. Exposing all grid points on the hologram plane, FP-HS is obtained.

In this system, thick holographic medium is used, about 10μm in the following experiment. Thus volume hologram is recorded, and due to the wavelength selectivity of volume hologram, monochromatic image is reconstructed even with white light illumination. Using red, green, and blue lasers, full-color images can be also recorded.

In the reconstruction of hologram, the hologram is illuminated by white light, ideally plane wave, and all elementary holograms simultaneously reproduce 2D images, as shown in fig.4. Each elementary hologram reproduces light-rays traveling to different directions from the location of the grid point. Then the light-field is reconstructed, and a viewer can see the reproduced image as if there were real objects.

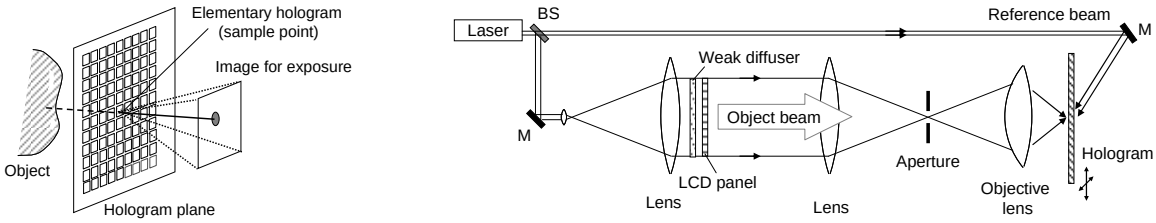

(a) (b)

Fig.3 (a) The geometry of calculating the image for exposure. (b) The optical system for FP-HS recording. BS: beam splitter, M: mirror. The hologram recording material is set to a XY translation stage to move horizontally and/or vertically after each exposure.

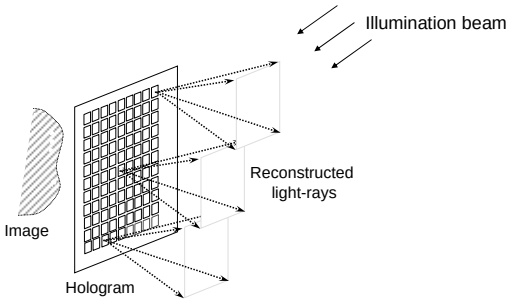

Fig.4 Reconstruction of FP-HS. Every elementary hologram reconstructs light-rays of different directions. Light-filed is reproduced as all elementary holograms are illuminated simultaneously.

Fig.5 Example of reconstructed image. The size and pitch of elementary hologram are both 50μm.

Fig.5 shows an example of reproduced images. As the resolution of the image for exposure was 100x100, the images of 10,000 different views in each elementary hologram cell, In addition to the binocular parallax, the motion parallax is correctly perceived with changing the viewing position, both horizontally and vertically. The depth perception is very natural reproduced image was clear.

3.3 Full-parallax 3D image scanning for high-density light-field reproduction of a real scene

The image presented above were generated by artificial computer graphics, but it is also expected to produce the holograms of pictured real objects. In HPO case, shooting images for HPO HS is not so difficult with using horizontal camera motion or horizontal camera array [4,13]. On the other hand, capturing full- parallax images requires much effort, and it has been difficult to make FP HS's of real objects. It is possible to apply model-based rendering using 3D shape and texture measurements, to reduce the complexity in FP image capturing. However, for the reproduction of high-fidelity realistic image, capturing and modeling of angular dependent reflection turn out to be complicated, and the problems due to occlusion often affect 3D images as well. There have been advanced reports on the light field acquisition recently [16,17], but the system becomes massive or complicated for capturing light field in real time. In this paper, a relatively simple system for capturing FP still-images is introduced, with a scanning vertical camera array.

In the proposed system, a vertical camera array is scanned horizontally as shown in fig.6(a), and vertical parallax information is interpolated from the captured data. Then only a small number of cameras are required, which allows relatively simple and compact implementation. To obtain high-density light-ray information, the rays passing through the gap between cameras are interpolated. In the system of fig.6, since the horizontal parallax information is captured in high-resolution, the depth of an object can be estimated at each pixel without much difficulty. With the depth

information at each pixel, vertical views between cameras are interpolated by depth image-based rendering (DIBR) technique [18].

In the experiment, FP 3D image captured by the proposed system was employed to synthesize full-color FP HS. The experimental system consists of seven compact CCD cameras (Point Gray Research, Flea) [Fig.6(b)] connected to PC through IEEE1394 interface, and a translation stage (Sigma, SGSP601200 (X)), which is also controlled by the same PC. The system is rather simple and concise, as a single PC can control the entire system. 600×7 images were captured in the experiment, where the horizontal pitch of the camera images was 0.8mm. Depth estimation using EPI analysis was done using about ±50 images for each camera around the target image. Then 271 vertical views were generated by interpolation, that is, FP 3D images with 600×271 views are obtained. Then the images for exposure were calculated, and an FP HS consisting of 280×200 elementary holograms, each of which reproduces light-rays of 100×100 directions was recorded. Good-quality 3D image of real object was observed as shown in Fig.6(c).

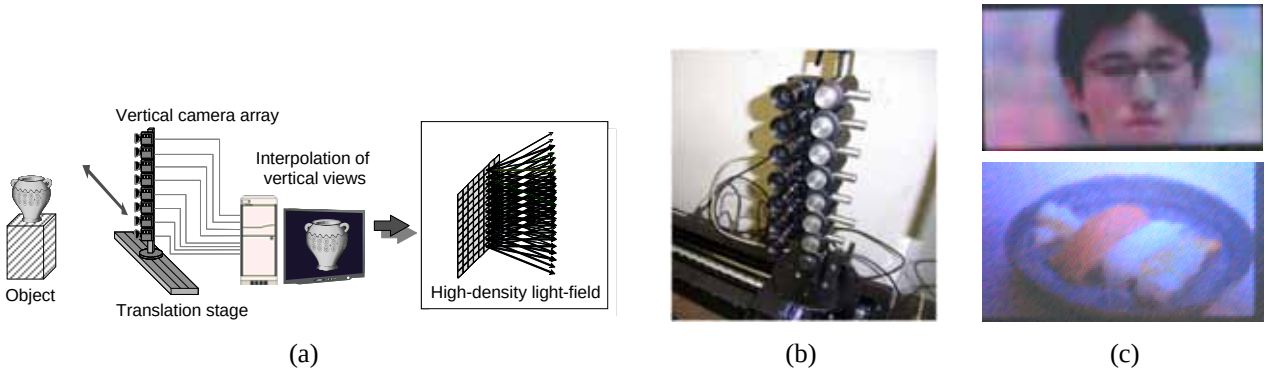

Fig.6 (a) Scanning vertical camera array system for the acquisition of high-density light field information. (b) Experimental of vertical camera array. (c) Reconstructed images. Upper: human face, and lower: "sushi."

3.4 Full-parallax holographic stereogram as a ray-to-wavefront converter

The optical arrangement shown in fig.3 is a Fourier transform system, and elementary holograms are the Fourier transform holograms of the image for exposure. This means that the wavefront reconstructed from FP-HS is a superposition of the sets of wavefronts from elementary Fourier holograms. The difference of wavefront reproduced by HS and Fresnel hologram was analyzed in refs. 8 and 19. The phase information of the wavefront from HS only retains the information of the direction of wave propagation, while a coherent hologram reconstructs the phase of spherical wave that depends on the distance from the point light source. Another point is the sampling; the wavefront of HS is sampled on the hologram plane by elementary holograms. It was shown to be possible to add phase information that depends on the object depth, called phase added stereogram, resulting in the good approximation of the wavefront from Fresnel hologram if the sampling pitch is enough high. Even though HS lacks some phase information, it could be also considered to be an approximation of real hologram, if the error due to loss of the phase information is sufficiently small. From this point of view, it can be said that HS converts a set of light-rays to the wavefront. The influences of the sampling and the lack of some phase information in HS are discussed in the next subsection.

3.5 The limitation of ray-based approach

The limitation of the light-field display based on ray reproduction can be derived from the above discussion on the conversion from ray to wavefront. Namely, light-rays are sampled, and some phase information is lost. If we consider a plane on which the light-rays are sampled (RS plane) as shown in fig.7, the angular resolution of light-rays and the lateral resolution are limited by the sampling effect. Moreover, the elementary hologram act as an aperture, and the diffraction at the aperture causes decrease of angular resolution. This affects the reconstructed image; image blur and artifact due to the diffraction appear. The influence of figs.7 (b) and (c) increases in proportion to the distance of the image from the RS plane.

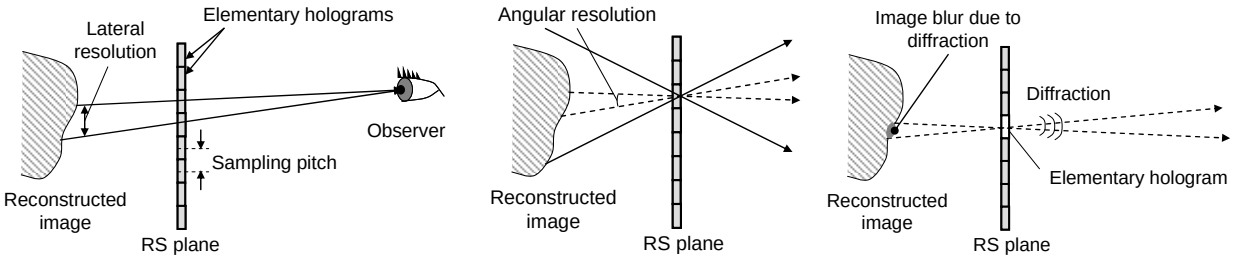

(a) (b) (c)

Fig.7 The limitation of ray-based approach in resolution. (a) The lateral resolution is limited by the sampling on the RS plane. (b) The angular resolution of light-rays is determined by the sampling of light-rays. (c) The angular resolution is also degraded by diffraction at the elementary hologram. In this case the size of an elementary hologram is considered to be the aperture size that causes the diffraction effect.

4. WAVEFRONT-BASED HOLOGRAPHIC DISPLAY CALCULATED FROM RAY-INFORMATION

4.1 CGH calculation for electro-holographic 3D display

Holography reproduces coherent light-field and is expected to be employed for ultra-high quality 3D display in future. To realize electro-holographic 3D display, the method for calculating hologram pattern is a crucial issue in addition to the advancement of display device. Many papers have been devoted to this issue. A typical method among them defines a set of numerous point light sources on the object surface, and superposes the spherical waves from those point sources on the hologram plane. It is called point-source method (PSM) hereafter. PSM is capable of reconstructing high-resolution image even in the image that is distant from the hologram plane, since the light propagation is correctly simulated. Polygon-based method was also proposed and excellent image reproduction has been achieved [20].

However, if we remind advanced rendering techniques in computer graphics, the limitation of conventional techniques for CGH calculation is obvious. In response to this problem, there have been also proposed methods for CGH calculation that can utilize the techniques of conventional computer graphics [7,8]. It is based on the principle of HS (called HS-CGH in this paper). A set of parallax images is calculated using rendering technique of computer graphics, and taking the Fourier transform of each parallax image, the wavefront on the hologram plane can be derived as explained in 3.3. It is possible to obtain CGH of realistic 3D image by exploiting variety of conventional rendering techniques in this method. Nevertheless it should be noted that the image resolution is limited if the image location is distant from the hologram plane, as explained in 3.5.

Since the important feature of holographic display is the capability of reproducing very deep 3D image in high-resolution, as is presented in section 2, both methods explained above are not satisfactory for realistic 3D display. The method proposed in our recent paper [9] is aiming at taking the merits of those wavefront-based and ray-based approaches. The details of the proposed method are given below.

4.2 CGH calculation method using ray-sampling plane

In the proposed method for CGH calculation, a rectangular window is defined near the object location, and the light-rays that pass through the window plane are derived using rendering technique of computer graphics. The window is called ray-sampling (RS) plane. As shown in fig.8, the light-field is sampled on the RS plane. If the RS plane is located near the object, the degradation due to the ray sampling and the diffraction effect can be kept satisfactory small, according to the discussion in 3.5. Thus locating the RS plane near the object, it is possible to avoid the decrease of resolution. The sampled light-field is converted to wavefront by taking Fourier transform of the angular distribution of light-ray intensity, as explained in 3.4. Random phase pattern is attached to the image before the Fourier transform so as to keep the intensity variation small on the RS plane. Then, the wavefront propagation from the RS plane to the final hologram is calculated by Fresnel transform, and the hologram fringe is obtained by interfering with the virtual reference wave.

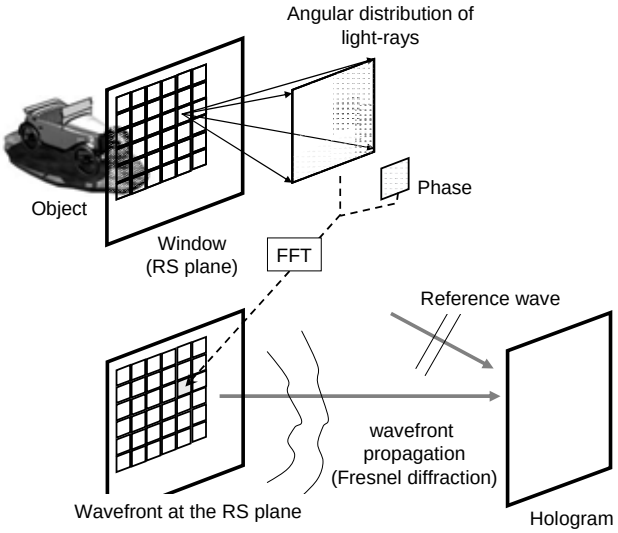

Fig.8 The schematic diagram of CGH calculation technique using RS plane. In the upper figure, the angular distribution of light-rays is collected at each sampled point on the RS plane. The ray information is Fourier transformed after the random phase modulation, yielding the wavefront of a small area on the RS plane [lower figure]. After all the ray information is transformed, the obtained wavefront is Fresnel transformed to derive the wavefront on the hologram plane.

The features of the proposed method are summarized as follows;

- High-resolution sampling is possible even for the objects distant from the display plane, since the light-rays are sampled near the objects.
- Image blur or artifact due to diffraction does not affect the reconstructed image because the propagation from the RS plane to the hologram is calculated based on diffraction theory.
- If the RS plane is defined in parallel to the hologram plane, the distance of wave propagation is constant, and high-speed computation of Fresnel diffraction can be implemented by using FFT (Fast Fourier Transform).
- The hidden surface removal, which is one of challenging task in CGH calculation for 3D display [21-23], can be easily done by ray-tracing in conventional computer graphics. Various other techniques for rendering can be applied as well, such as texture mapping, specular reflection, shadow, etc.
- It is easy to apply the method to real-world objects using IBR technique, with roughly estimating the range of the object depth.

When there are objects at different depths, for example, background and foreground objects, we can define different RS planes for respective objects. In fact, occlusion processing is required for the objects registered to different RS planes, as is described in the next subsection. Also by defining plural RS planes, the synthesis of different objects, or artificial and real objects becomes possible. Therefore the method seems to be suitable for holographic display of realistic image of deep 3D scene.

Some issues are still unsolved in the proposed method, for example, when the object is continuous in depth direction, it is difficult to define an RS plane parallel to the hologram plane. Another issue to be addressed is a fast computation; the algorithm can be improved to reduce the computational cost, and the implementation such as the use of GPU or parallel processing should be studied.

4.3 Occlusion processing using ray-sampling planes

The occlusion processing is one of the tough issues in the calculation of hologram [21-23]. In the proposed method, self occlusion, some surfaces are hidden by other surfaces of the same object, can be directly achieved by the rendering technique. Another type of occlusion, mutual occlusion between different objects, should be dealt with by defining an RS plane for each object located at different depth, as shown in fig.9. The wavefront propagation from the first RS plane to second one is first calculated by Fresnel transform to derive the wavefront on the second RS plane, and is converted to the ray-information using inverse Fourier transform on the second RS plane. Then the occlusion processing is easily realized in the light-ray domain. The ray-information after the occlusion processing is converted to the wavefront again, and the Fresnel transform leads the wavefront on the hologram plane.

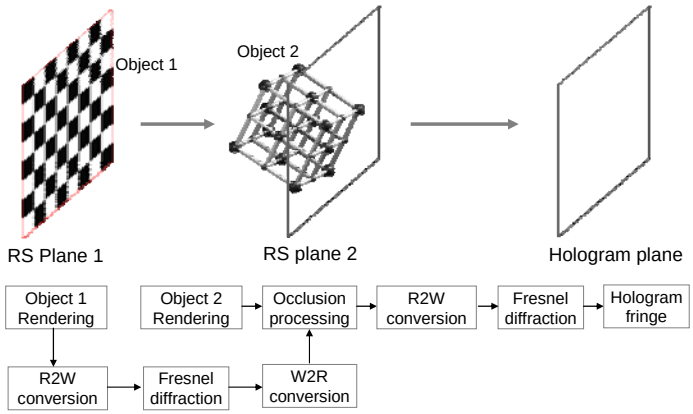

Fig.9 Schematic diagram of the proposed method incorporating the mutual occlusion processing. R2W and W2R represent ray-to-wavefront and wavefront-to-ray transformations, respectively.

4.4 Experiment

First the reconstructed image of the proposed method was compared with that of ray-based method (HS-CGH) by numerical simulation. In this case a 2D object was defined and located 200 mm behind the hologram plane. The number of angular sampling was 32×32 in both HS-CGH and proposed method. The number of sampling grid points on the RS plane in the proposed method was 128×128, and the same number of sample points was assigned on hologram plane in case of HS-CGH. An RS plane was placed 5mm front of the object. Total number of pixels in CGH was 4096x4094 in both cases. Fig.9 shows the simulated reconstructed images by the proposed and HS-CGH. It can be confirmed that high-resolution image was reproduced by the proposed method, while the image reconstructed by ray-based hologram was blurred to large extent.

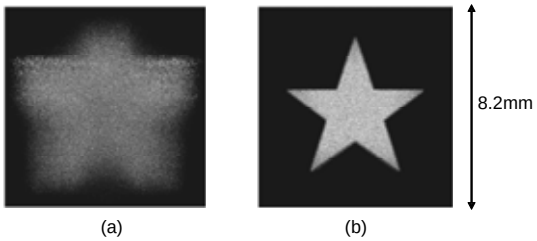

Fig.10 Simulation result. (a) Reconstructed image by ray-based hologram. (b) Reconstructed image by proposed method. The hologram is in 4096×4096 pixels where the number of ray-sampling points is 128×128.

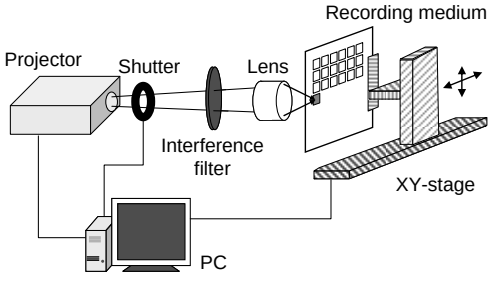

Fig.11 Optical setup of CGH printer.

In the next step of experiment, we calculated CGH based on the proposed technique and the image reconstruction was tested using a CGH printer developed for this purpose. Fig. 11 shows the setup of the CGH printer system. The image displayed by a DLP projector (Marantz, Model VP-12S2) whose projection lens was removed was formed a reduced image on the recording material. Since the resolution of a spatial light modulator in the projector is not enough for holographic display, hologram pattern is divided into sub-images, which are recorded sequentially. For this purpose, the recording material is set to a XY pulse-controlled translation stage, and after an exposure the material is moved to the next position for the exposure. The number of pixels of the spatial light modulator (DMD) was 1280x720, and the reduced image size and the pixel pitch on the hologram plane were about 2.6×1.4mm and 2μm, respectively. To reduce the influence of chromatic aberration, an interference filter of 460nm was placed in the system. The system was similar to the "fringe" printer previously reported [24], except that the incoherent light source of the projector was used, instead of a laser source used in the fringe printer.

The first object is a car, and the images of different views were calculated by using commercial rendering software. Then the images of angular ray-distribution were calculated based on IBR technique. The hologram size was 50mm, and the object is located 200mm behind the hologram plane. The calculated CGH pattern was exposed onto a holographic

recording material using the above fringe printer. The reconstructed image of the hologram calculated by the proposed method is shown in fig.12 (a). It can be observed that the surface reflection property is exhibited by the technique of graphics rendering.

In addition, two objects, front and background, were also printed by the proposed method, with the occlusion processing described in 4.3. The arrangement of the object was the one shown in fig.9. RS planes were defined at 100mm and 150mm behind the hologram plane, the background object was located on the RS plane. The hologram size and resolution were 50mm×50mm and 16,384×16,384 pixels. Figs.12 (b) and (c) show the reconstructed images with changing the focusing position. Both the self and mutual occlusions were represented correctly as well as the focusing to each object was possible.

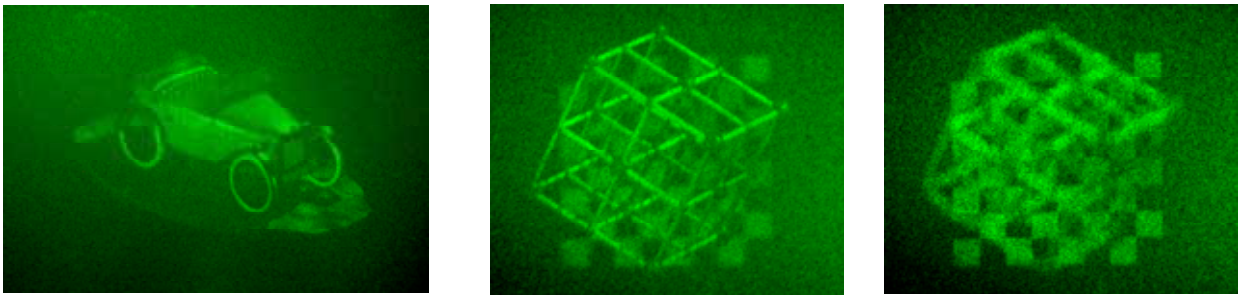

(a) (b) (c)

Fig. 12 Results of optical reconstruction of the hologram calculated by the proposed method. (a) The image that have glossy surface and shadows. (b) (c) The case of using two RS planes [see fig.9]. The camera focus was adjusted to front object in (b) and background object in (c).

5. SUMMARY

In summary, the light-field displays based on light-rays and wavefront are developed. The ray-based display is suitable for hardcopy, since under white light illumination, the angular resolution is not very high. On the other hand, for electro-holographic display, realistic reproduction of deep 3D scene is expected. So exploiting the conversion between the light-rays and wavefront, a CGH calculation method using RS plane is proposed. It becomes possible to employ the advanced rendering techniques for computer graphics in the computation of hologram, and it enables the improved occlusion processing and the surface shading for the display of deep 3D image in high resolution. The hologram computation of more complex scene, such as objects around an areal plane, is a future issue. The reduction of speckle noise is also another topic that should be addressed for high-quality 3D display by holography.

This work was partly supported by the JSPS Grant-in-Aid for Scientific Research #17300032, and Toppan Printing Co. The author wish to thank Koki Wakunami, Hiroaki Yamashita, Ryota Kojima, in Tokyo Institute of Technology, and Shingo Maruyama, Toppan Printing Co., for providing experimental data.

REFERENCES

[1] M. Levoy and P. Hanrahan, "Light field rendering," Computer Graphics (Proc. SIGGRAPH'96), 31-42, (1996)
[2] M. Yamaguchi, N. Ohyama, and T. Honda, "Holographic 3-D printer," Proc. SPIE, 1212, 84-90 (1990)
[3] S. Maruyama, Y. Ono, and M. Yamaguchi, "High-density recording of full- color full-parallax holographic stereogram," Proc. of SPIE, 6912, 69120N-1-10 (2008)
[4] D. J. DeBitetto, " Holographic panoramic stereograms synthesized from white light recordings," Appl. Opt., 8, 8, 1740-1741 (1969)
[5] J. P. Waters, "Holographic image synthesis utilizing theoretical methods," Appl. Phys. Lett. 9, 405–407 (1966).
[6] A. D. Stein, Z. Wang, and J. J. S. Leigh, "Computer-generated holograms: a simplified ray-tracing approach," Comput. Phys. 6, 389–392 (1992).

[7] P. W. McOwan, W. J. Hossack and R. E. Burge, “Three-dimensional stereoscopic display using ray traced computer generated holograms,” Opt. Comm., Vol.82, No.12, 6-11 (1993).
[8] M. Yamaguchi, H. Hoshino, T. Honda, and N. Ohyama, "Phase added stereogram: calculation of hologram using computer graphics technique," Proc. SPIE, 1914, 25-31 (1993)
[9] K. Wakunami and M. Yamaguchi, "Calculation of computer-generated hologram for 3D display using light-ray sampling plane", Proc. SPIE 7619, 76190A (2010)
[10] S. Bains, " The rise and rise of the holographic printer," OE Reports, SPIE, May (1996)
[11] M. Halle, S. A. Benton, M. A. Klug, J. Underkoffler, "The Ultragram: A generalized holographic stereogram," Proc. SPIE, Vol. 1461, 142-155, (1991).
[12] W. C. Spierings and E. van Nuland, "Development of an office holoprinter II", Proc. SPIE 1667, 52 (1992)
[13] A. Shirakura, N. Kihara, S. Baba: "Instant Holographic Portrait Printing System," Proc. SPIE, Vol. 3293, 1998
[14] M. A. Klug, A. Klein, W, J. Plesniak, A. B. Kropp, B. Chen, "Optics for full-parallax holographic stereograms," Proc. SPIE, Vol. 3011, 78-88 (1997)
[15] M. Yamaguchi, H. Higuchi, R. Kojima, and S. Maruyama, "Evaluation of Light-Ray Reproducibility in Full-Parallax Holographic Stereogram," in Digital Holography and Three-Dimensional Imaging, OSA Technical Digest, paper DTuA4 (2007)
[16] B. Wilburn, N. Joshi, V. Vaish, E.-V. Talvala, E. Antunez, A. Barth, A. Adams, M. Horowitz, M. Levoy, "High performance imaging using large camera arrays," ACM Trans. Graphics, Vol. 24, 3, 765-776 (2005)
[17] M. Brewin, M . Forman, and N. A. Davies, "Electronic capture and display of full-parallax 3D images," Proc. SPIE, Vol. 2409, 118-124, (1995)
[18] L. Zhang, "Stereoscopic image generation based on depth images for 3D TV," IEEE Trans. Broadcasting, Vol. 51, 2, 191-199 (2005)
[19] M. Yamaguchi, N. Ohyama, T. Honda, “Imaging characteristics of holographic stereogram,” Japanese J. of Optics, (Kogaku), Vol. 22, 11, 714-720 (1993) (in Japanese).
[20] K. Matsushima and S. Nakahara, "Extremely high-definition full-parallax computer-generated hologram created by the polygon-based method," Appl. Opt. 48, H54-H63 (2009)
[21] P. St-Hilaire, S. A. Benton, M. E. Lucente, M. L. Jepsen, J. Kollin, H. Yoshikawa and J. S. Underkoffler, "Electronic display system for computational holography", Proc. SPIE 1212, 174 (1990)
[22] J. S. Underkoffler, “Occlusion processing and smooth surface shading for fully computed synthetic holography,” Proc. SPIE, Vol.3011, 53-60, (1997) .
[23] K. Matsushima, “Exact hidden-surface removal in digitally synthetic full-parallax holograms,” Proc. SPIE, Vol.5742, 25-32 (2005).
[24] H. Yoshikawa, K. Takei, "Development of a compact direct fringe printer for computer-generated holograms," Proc. SPIE 5290, 114-121 (2004)